



PTPN2 regulates the activation of KRAS and plays a critical role in proliferation and survival of KRAS-driven cancer cells

Received for publication, September 18, 2019, and in revised form, October 12, 2020. Published, Papers in Press, October 29, 2020, DOI 10.1074/jbc.RA119.011060

Zhangsen Huang[‡], Mingzhu Liu[‡], Donghe Li, Yun Tan, Ruihong Zhang, Zhizhou Xia[Ⓜ], Peihong Wang, Bo Jiao, Ping Liu^{*}, and Ruibao Ren^{*}

From the Shanghai Institute of Hematology, State Key Laboratory for Medical Genomics, National Research Center for Translational Medicine at Shanghai, Collaborative Innovation Center of Hematology, Ruijin Hospital affiliated to Shanghai Jiao Tong University School of Medicine, Shanghai, China

Edited by Alex Tokor

RAS genes are the most commonly mutated in human cancers and play critical roles in tumor initiation, progression, and drug resistance. Identification of targets that block RAS signaling is pivotal to develop therapies for RAS-related cancer. As RAS translocation to the plasma membrane (PM) is essential for its effective signal transduction, we devised a high-content screening assay to search for genes regulating KRAS membrane association. We found that the tyrosine phosphatase PTPN2 regulates the plasma membrane localization of KRAS. Knockdown of PTPN2 reduced the proliferation and promoted apoptosis in KRAS-dependent cancer cells, but not in KRAS-independent cells. Mechanistically, PTPN2 negatively regulates tyrosine phosphorylation of KRAS, which, in turn, affects the activation of KRAS and its downstream signaling. Consistently, analysis of the TCGA database demonstrates that high expression of PTPN2 is significantly associated with poor prognosis of patients with KRAS-mutant pancreatic adenocarcinoma. These results indicate that PTPN2 is a key regulator of KRAS and may serve as a new target for therapy of KRAS-driven cancer.

RAS proteins are small GTPases that regulate diverse cellular processes, including proliferation, differentiation, migration, apoptosis, and senescence (1). Mammalian cells mainly express three RAS genes that encode four highly homologous proteins: HRAS, NRAS, KRAS4A, and KRAS4B. KRAS4A and KRAS4B result from an alternative splicing at the C terminus of the KRAS gene (2). Because KRAS4B is the predominant splice variant of KRAS, it is referred to as KRAS hereafter.

RAS genes are the most frequently mutated oncogene in cancer, nearly 20–30% of human malignancies carry RAS gene mutations. Among the RAS gene family, KRAS is the most commonly mutated, which occurs in 71% of pancreatic, 29% of colorectal, and 18.6% of lung carcinomas (3). It has been shown that mutated KRAS not only plays pivotal roles in cancer initiation (4–6), but also contribute to several hallmarks of human cancer (7, 8). Moreover, inhibition of activated KRAS could delay tumor progression both *in vitro* and *in vivo* (9–11). These

observations prompted many groups to target either mutant KRAS directly or downstream effectors.

Thus far, directly targeting oncogenic KRAS only succeeded in one certain form, KRAS^{G12C} (12, 13), which comprises only 12% of KRAS mutations in all human cancers, so it is still needed to develop new target molecules for other oncogenic KRAS. Inhibiting protein–protein interactions and KRAS localization are novel approaches to target mutant KRAS and block oncogenic KRAS signaling (14–16), although the efficacy in clinical is still unknown. Targeting the KRAS effector signaling pathways could also prove efficacious in treating tumors with KRAS mutations, as the inhibitors have entered clinical trials demonstrating promising clinical activity in KRAS mutant tumor (17, 18). However, toxicities associated with their sustained inhibition, variable responses rates, and acquired adaptive resistance due to the activation of other kinases are limiting the efficacy and the clinical progression of these compounds as monotherapy treatment (19–21). Hence it remains an urgent need to identify new target strategies to block oncogenic KRAS signaling. KRAS interacts with downstream effectors only when it associates with the plasma membrane (PM) (14, 22–24), so inhibition of KRAS localization is a valid therapeutic approach to block signal transmission by oncogenic KRAS.

KRAS is synthesized as cytosolic proteins and gains affinity for the PM through post-translational modification of its carboxyl terminal CAAX motif (CVIM sequence) by farnesyltransferases (FTase) or geranylgeranyltransferase (GGTase), followed by cleavage of the VIM residues by RAS converting enzyme 1 (RCE1) and methyl esterification of the farnesylated cysteine residue by isoprenylcysteine carboxyl methyltransferase (ICMT) (22). Given the critical role of prenylation for KRAS membrane association and neoplastic transformation, and farnesylation of KRAS by FTase is the first step in the KRAS post-translational modification, FTase is the ideal target for KRAS-driven cancers. However, FTase inhibitors (FTIs) failed to show high efficacy as expected in clinic (25). The main reason is that KRAS protein can undergo alternative prenylation by GGTase in the presence of FTIs (26). Inhibitors targeting FTase and GGTase in combination have been proved too toxic to be clinically useful (27).

Despite the clinical failure of FTIs, inhibition of KRAS–PM interactions remains an attractive therapeutic approach to abrogate the KRAS oncogenic activity (14, 28–31). Here we devised a high-content screening assay and carried out an

This article contains supporting information.

[‡]These authors contributed equally to this work.

^{*}For correspondence: Ruibao Ren, ren@brandeis.edu; Ping Liu, liupingjize@126.com.

Present address for Zhangsen Huang: Scientific Research Center, The Seventh Affiliated Hospital, Sun Yat-sen University, Shenzhen, China.

This is an Open Access article under the [CC BY](https://creativecommons.org/licenses/by/4.0/) license.

PTPN2 is important for KRAS-driven cancer

siRNA screening to identify key molecules required for oncogenic KRAS plasma membrane association. We show that, for the first time, protein-tyrosine phosphatase non-receptor type 2 (PTPN2) regulates the KRAS plasma membrane association and plays an important role in KRAS-dependent cancer cell proliferation and survival. Mechanistic studies demonstrate that PTPN2 negatively regulates tyrosine phosphorylation of KRAS, which, in turn, affects the activation KRAS and its downstream signaling. Our data suggest that PTPN2 could serve as a potential therapeutic target for KRAS-driven cancer.

Results

Identification of PTPN2 as a regulator for KRAS plasma membrane association by an siRNA screening

To identify genes required for KRAS membrane trafficking, we developed an image-based screening assay that monitors the degree of KRAS^{G12D} membrane association (Fig. 1A). To this end, we established a GFP-fused KRAS^{G12D} (GFP-KRAS^{G12D}) human embryonic kidney (HEK) 293T cell line stably expressing GFP-KRAS^{G12D}. We found that the majority of GFP-KRAS^{G12D} proteins are localized to the PM (Fig. 1B). We then screened a 147-siRNA sublibrary enriched with targets that regulate protein translocation, using an Opera Phenix High-Content Screening System (the siRNA-target genes and sequence was listed in Table S1). The PDE6D siRNA was used as a positive control. After cells were treated with arrayed siRNAs for 72 h in 96-well-plates, one siRNA, PTPN2 siRNA, significantly changed the ratio of PM-bound GFP-KRAS^{G12D} over cytosolic GFP-KRAS^{G12D} (Fig. 1B).

We used additional PTPN2 siRNA, as well as KRAS siRNA, from GenePharma to confirm the screening result. Two different PTPN2 siRNAs (PTPN2 siRNA-432 and PTPN2 siRNA-1161) could effectively decrease the level of PTPN2 in GFP-KRAS^{G12D} HEK 293T cells (Fig. 1C). We then checked the level of GFP-KRAS^{G12D} on the PM using a membrane protein extraction kit, and found that silencing PTPN2 reduced the translocation of KRAS^{G12D} to the PM by approximately 30% compared with the negative control (NC) (Fig. 1, D and E). Meanwhile, the level of KRAS^{G12D} in the cytoplasm was slightly increased (Fig. 1, D and E). These data suggest that PTPN2 plays an important role in regulating the plasma membrane association of KRAS^{G12D}.

PTPN2 is required for KRAS-dependent tumor cell growth

We next investigated the effect of PTPN2 on cancer cell growth, using pooled siRNAs to knockdown PTPN2 in a panel of five mutant KRAS-harboring human cancer cell lines (H460, PaTu8988T, HCT-116, A549, and DLD-1) and two KRAS wild-type human cancer cell lines (HT-1080 and SK-MEL-30). Pooled siRNAs to knockdown KRAS were used as a positive control. Cells were treated with siRNAs for 72 h, followed by the CellTiter-Glo[®] luminescent cell viability assay. As shown in Fig. 2A, silencing PTPN2 with pooled siRNAs markedly attenuated the proliferation of H460 (lung), PaTu8988T (pancreatic), HCT-116 (colon), and HT-1080 (fibrosarcoma) cells, and slight but significantly growth inhibition of A549 (lung) and SK-MEL-30 (skin). However, it is not the case in DLD-1 (colon)

cells. Interestingly, the growth inhibitory effect of knocking down PTPN2 was consistent with that of knocking down KRAS (Fig. 2A), suggesting that PTPN2 plays a critical role in KRAS oncogenic signaling. Accordingly, DLD-1, which is KRAS-independent, was less sensitive to the knockdown of either PTPN2 or KRAS (Fig. 2A). Both two pooled siRNAs effectively decreased the expression of PTPN2 and KRAS in all seven cell lines (Fig. 2B).

We further confirmed the effect of PTPN2 on the three mutant KRAS-dependent cell lines by using two different siRNAs, respectively. Both siRNAs were found to reduce the expression of PTPN2 and suppress the proliferation of the cell lines (Fig. 2, C and D).

PTPN2 is required for KRAS-dependent tumor cell survival

For more accurate detection of cell proliferation, we examined the effect of PTPN2 and KRAS knocking down on cell proliferation by a BrdU assay. Consistent with the results of CellTiter-Glo[®] luminescent cell viability assay, the fraction of BrdU-positive cells was significantly decreased in all these cell lines described above except for DLD-1 (Fig. 3A). It is notable that the effect of PTPN2 knockdown is less than that of KRAS knockdown in H460, PaTu8988T, and A549, suggesting that PTPN2 has limited activity on the proliferation signaling of KRAS in these cells.

We also examined the effect of PTPN2 on cell survival. All these tumor cell lines described above were treated with PTPN2, KRAS, or control siRNAs for 72 h, followed by staining with Annexin V-APC and propidium iodide. Flow cytometric analysis showed that the percentage of apoptosis in these KRAS-dependent tumor cell lines was significantly higher than that of controls (Fig. 3B). The effect of PTPN2 knockdown is no less than that of KRAS knockdown in KRAS-dependent tumor cell lines, suggesting that PTPN2 is required for the cell survival signaling of KRAS.

PTPN2 regulates the activation of oncogenic KRAS and its downstream signaling

To gain insights into the mechanism by which PTPN2 regulates the proliferation and survival of KRAS-dependent tumor cells, we first checked whether PTPN2 affects the KRAS activation, using an RAS-GTP pull-down assay. As shown in Fig. 4A, the level of GTP-KRAS^{G12D} was significantly decreased in GFP-KRAS^{G12D} expressing 293T cells treated with PTPN2 siRNA, either pooled or two different single siRNAs, compared with that in GFP-KRAS^{G12D} expressing 293T cells treated with scrambled siRNA. Similarly, the level of GTP-bound KRAS in H460 cells was also decreased by treating with pooled PTPN2 siRNAs (Fig. 4B).

We next tested whether PTPN2 affects the activation of KRAS downstream signaling pathway. As shown in Fig. 4C, both KRAS and PTPN2 knockdown could dramatically decrease the phosphorylation levels of MEK and ERK in KRAS-dependent tumor cell lines HCT-116, PaTu8988T, and H460. Collectively, these data demonstrate that PTPN2 is required for the full activation of oncogenic KRAS and its downstream signaling pathway.

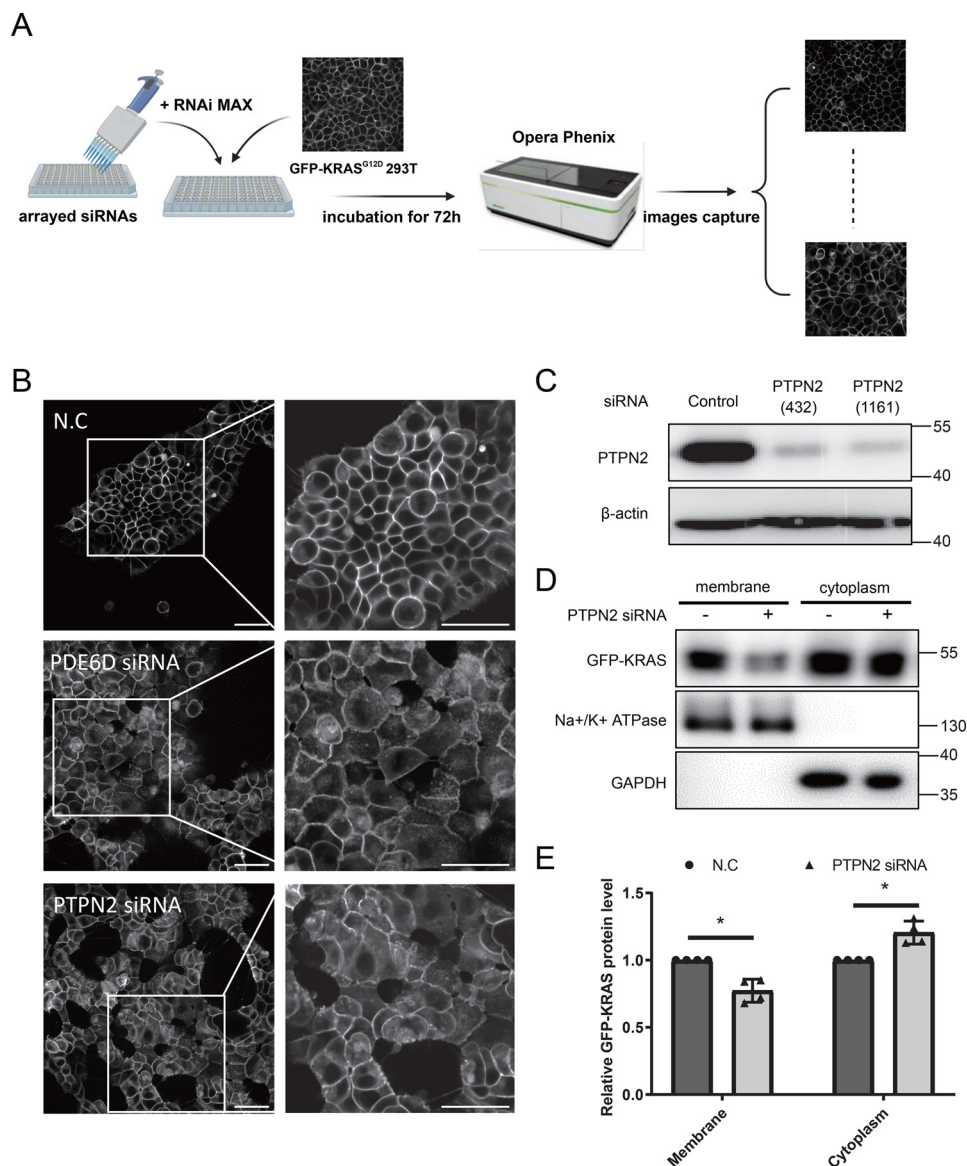


Figure 1. PTPN2 regulates KRAS membrane association. *A*, schematic representation of the screening. Arrayed siRNAs were transfected into GFP-KRAS^{G12D} 293T using RNAiMAX. After the 72-h incubation, images were acquired for 17 fields with a $\times 40$ water immersion objective using the GFP-confocal mode in an Opera Phenix High-Content Screening System. *B*, PTPN2 siRNA induced GFP-KRAS^{G12D} mislocalization. Representative images (GFP channel only) of GFP-KRAS^{G12D} HEK 293T cells transfected with PTPN2 smartpool ON-TARGETplus siRNAs. Scale bar: 50 μ m. *C*, Western blot analysis of the knockdown efficiency of PTPN2 in GFP-KRAS^{G12D} HEK 293T after transfection with the indicated siRNAs. The immunoblot data are representative of at least three independent experiments. *D*, GFP-KRAS^{G12D} HEK 293T cells were treated with pooled PTPN2 siRNAs or NC siRNA for 72 h. To detect exogenous GFP-fused KRAS proteins, membrane proteins, and cytoplasmic proteins were isolated, followed by Western blot analysis with an anti-GFP antibody. (Na⁺-K⁺)-ATPase was used as the input of membrane proteins control, and GAPDH was used as the input of cytoplasmic proteins control. *E*, quantitation of data in *C* are shown. Signal intensity was quantified for GFP-KRAS^{G12D} in the membrane fraction and cytoplasmic fraction ($n = 4$ independent biological experiments depicted as normalized intensity for siPTPN2 over the NC control; mean \pm S.D.; two-tailed *t* test. *, $p < 0.05$).

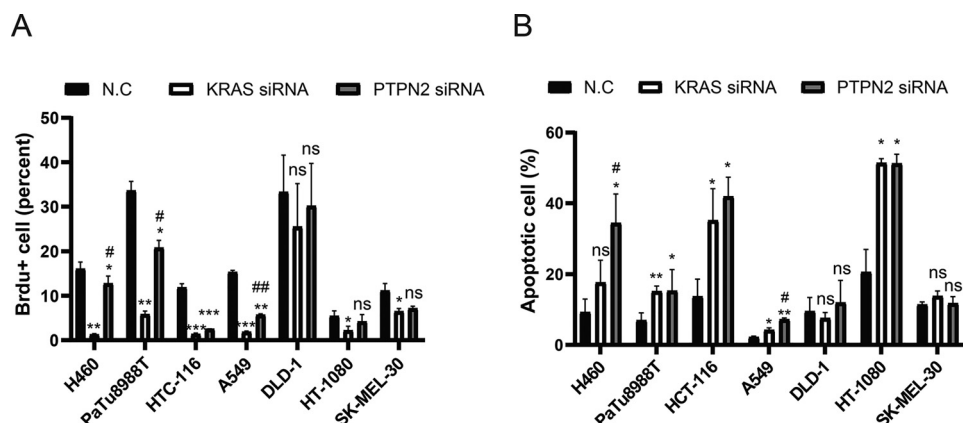
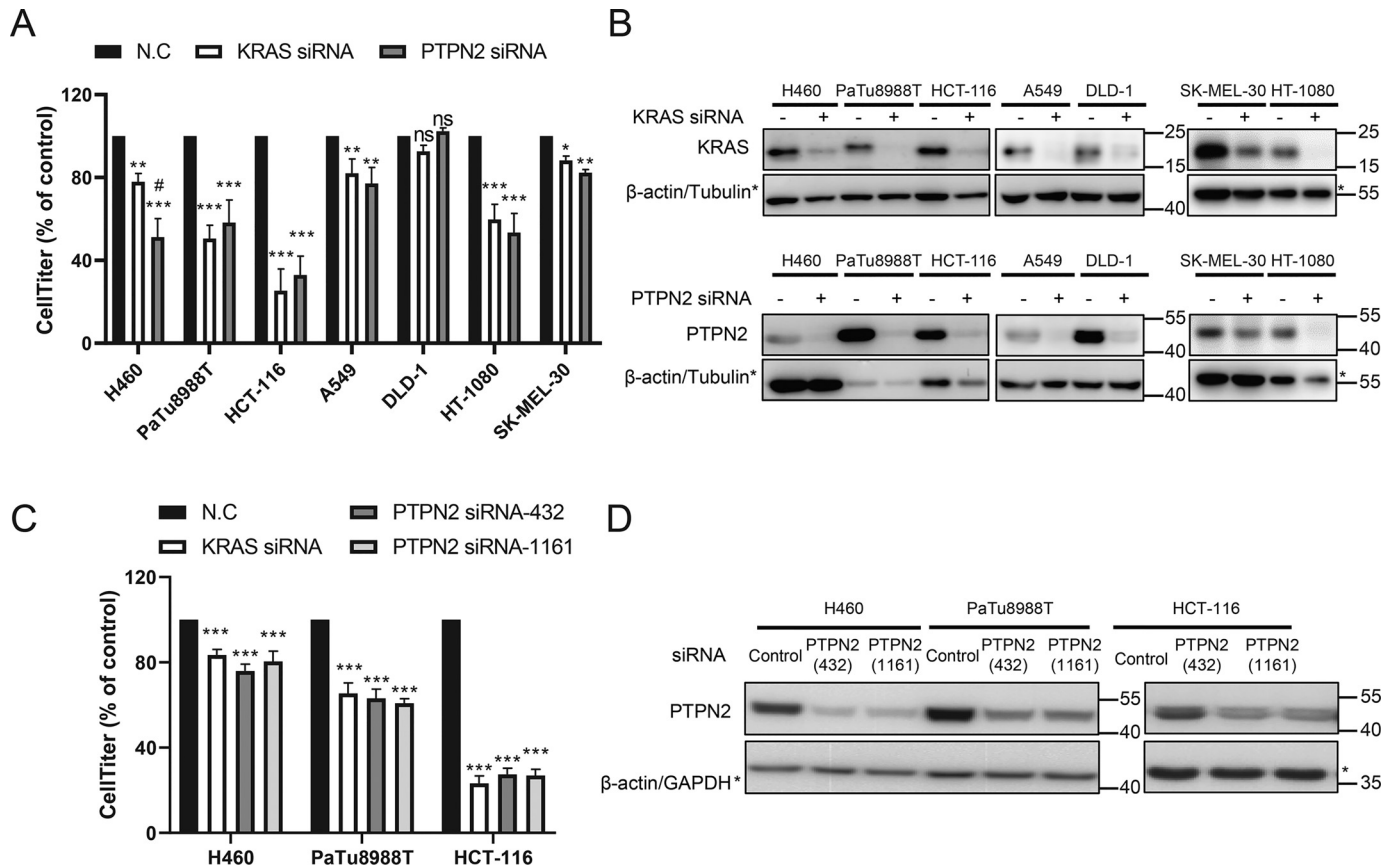
We also examined the protein stability of GFP-KRAS^{G12D} in HEK 293T cells in the presence of protein synthesis inhibitor cycloheximide (CHX, 50 μ g/ml). As shown in Fig. 5A, the endogenous KRAS protein was markedly susceptible to PTPN2 knockdown, whereas only a marginal change was noted for the exogenous GFP-KRAS^{G12D} protein. The different effects of PTPN2 on the stability between endogenous and exogenous KRAS may be partly explained by the exogenous KRAS is the mutant form, whereas the endogenous KRAS is the wildtype form. We also examined the effect of PTPN2 knockdown on half-life of the endogenous KRAS protein in the KRAS mutant cell line. We transfected cancer cells carrying KRAS-Q61K

(H460) mutant with either control or PTPN2 siRNA. As shown in Fig. 5, C and D, mutant KRAS half-life changed marginally in PTPN2 knockdown cells. Taken together, these data demonstrate that PTPN2 is not involved in maintaining mutant KRAS protein stability.

PTPN2 regulates the level of tyrosine phosphorylation of KRAS

It has been shown that tyrosine phosphorylation of KRAS reduces its signal transduction activity, whereas tyrosine-phosphorylated KRAS can be dephosphorylated by SHP2 (encoded

PTPN2 is important for KRAS-driven cancer



by PTPN11 (32). PTPN2 is a member of the PTP family and has been shown to dephosphorylate several tyrosine kinases. We tested whether PTPN2 regulates KRAS signaling through

dephosphorylating KRAS. Myc-KRAS^{G12D} HEK 293T cell lysates were immunoprecipitated with anti-Myc antibody followed by anti-pTyr immunoblot. We found the level of

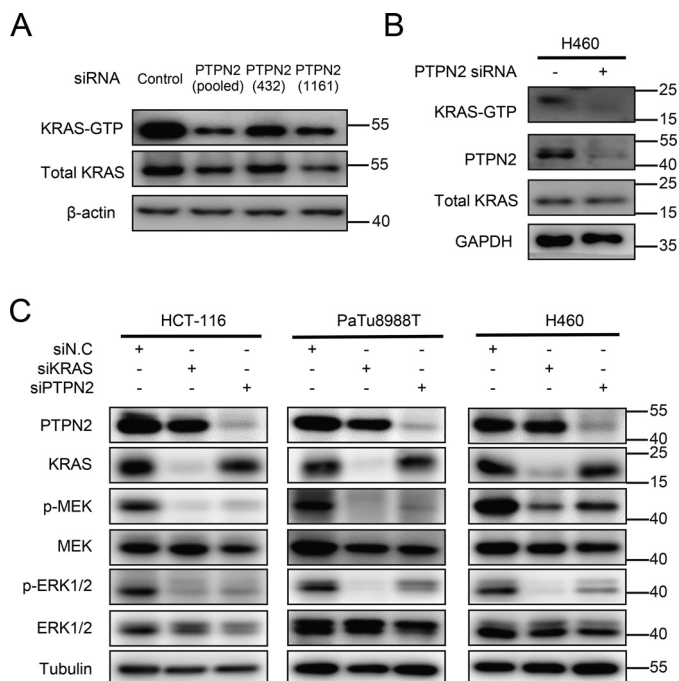


Figure 4. Effect of PTPN2 knockdown on the KRAS activation, signaling, and tyrosine phosphorylation. *A*, GFP-KRAS^{G12D} 293T cells were transfected with PTPN2 siRNA or NC and cultured for 72 h. Cellular lysates were prepared and the levels of RAS-GTP were determined. Pulldown of RAS-GTP was performed with RAF-RBD-agarose beads. Precipitates were immunoblotted using an anti-KRAS antibody (labeled KRAS-GTP). The input samples were immunoblotted with the identical antibodies. *B*, H460 cells were transfected with PTPN2 siRNA or NC and cultured for 72 h. Cellular lysates were prepared and the levels of RAS-GTP were determined. Pulldown of RAS-GTP was performed with RAF-RBD-agarose beads. Precipitates were immunoblotted using an anti-KRAS antibody (labeled KRAS-GTP). The input samples were immunoblotted with the identical antibodies. The immunoblot data are representative of two independent experiments. *C*, HCT-116, PaTu8988T, and H460 cells were transfected with PTPN2 siRNA, KRAS siRNA, or NC and cultured for 72 h. Cells were lysed and immunoblotted with the indicated antibodies. The immunoblot data are representative of three independent experiments.

phosphorylated KRAS in Myc-KRAS^{G12D} HEK 293T cells was significantly increased after knockdown of PTPN2 (Fig. 6, *A* and *B*). These results indicate PTPN2 is also a tyrosine phosphatase for KRAS. To confirm that the observed effect on KRAS phosphorylation was attributable specifically to PTPN2 knockdown, we generated two siRNA-resistant wildtype PTPN2 isoforms (PTPN2-1-R and PTPN2-2-R) and a phosphatase-inactive mutant (PTPN2-D182A) (Asp-182 changed to Ala) construct for rescue experiments (Fig. 6*C*). Transfection of PTPN2-1-R and PTPN2-2-R constructs into PTPN2 siRNA (1161)-treated cells markedly increased PTPN2 expression (Fig. 6*C*). More importantly, overexpression of PTPN2-2-Res but not PTPN2-2-D182A-Res, nor PTPN2-1-Res, decreased the level of tyrosine phosphorylation of KRAS (Fig. 6, *C* and *D*). This result indicates that PTPN2 regulates tyrosine phosphorylation of KRAS through its tyrosine phosphatase activity and that PTPN2-2-Res is the primary isoform to carry out this function.

High level PTPN2 expression is associated with poor prognosis of pancreatic adenocarcinoma

Our data show that PTPN2 plays an important role in the maintenance of KRAS-dependent tumor cells. To determine

the impact of PTPN2 expression in KRAS-related cancers, we analyzed clinical databases. We separated KRAS mutation, KRAS expression, PTPN2 expression, and clinical information of KRAS-related cancers from TCGA cohorts (Table S2). We first performed overall survival analysis to compare the survival of patients harboring mutant or wildtype KRAS in pancreatic adenocarcinoma (PAAD), lung adenocarcinoma (LUAD), and colorectal adenocarcinoma (COAD). As shown in Fig. 7*A*, KRAS mutation is associated with poor prognosis of PAAD, but not that of LUAD or COAD. We then analyzed the impact of PTPN2 on survival of patients containing KRAS mutations. As shown in Fig. 7*B*, high expression of PTPN2 is significantly associated with poor prognosis in KRAS-mutant PAAD patients ($p = 0.0058$), but not in patients with LUAD or COAD. In KRAS-WT patients, the high expression of KRAS mRNA is significantly associated with poor prognosis in PAAD ($p = 0.0112$) and LUAD ($p = 0.0105$) but not in COAD ($p = 0.1145$) (Fig. 7*C*). However, PTPN2 expression levels are not significantly associated with survival in KRAS high expression patients or KRAS low expression patients with PAAD ($p = 0.9121$ and $p = 0.2106$, respectively) (Fig. 7, *D* and *E*). These clinical data support our conclusion that PTPN2 plays an important role in KRAS-mutant-dependent tumors.

Discussion

It has been known that 20–30% human cancers, including a high percentage of pancreatic, lung, and colorectal cancers, are driven by mutations in KRAS. Genetically engineered mouse models have shown that *Kras* mutation could faithfully recapitulate the progression of the human cancer, and a mutated form of *Kras* is sufficient to initiate pancreatic and lung cancer (33, 34). Furthermore, silencing *Kras* with siRNA in these genetically engineered mouse models significantly prolonged the survival of mice (9–11). Although scientists have made great progresses in the last 3 decades toward understanding the KRAS signaling pathways, drug development in blocking KRAS function has been ineffective. Based on the fact that KRAS regulates signaling pathways for cell growth only when associated with the PM (14, 22–24), targeting KRAS membrane translocation has become an alternative approach. In this study, we screened a custom-designed siRNA library using an image based high-content screening. We found that PTPN2 is required for the effective PM localization of KRAS, and PTPN2 is required for KRAS-dependent cell survival and, to a lesser extent, proliferation. Mechanistically, PTPN2-negatively regulated KRAS tyrosyl phosphorylation. In addition, analysis of the data from TCGA, we found that high PTPN2 expression is associated with poor prognosis of KRAS-mutant PAAD patients.

PTPN2, also known as T cell protein-tyrosine phosphatase (TCPTP), is a non-receptor phosphatase that is ubiquitously expressed (35), and plays critical roles in T cell-mediated immunity and inflammation (36–38). The role of PTPN2 in tumors has just begun to be investigated in recent years. It has been reported that PTPN2 is frequently mutated and repressed in T-ALL, and further experiments reveal that PTPN2 negatively regulates the JAK/STAT signaling (39). Other studies have found that PTPN2 can act as an oncogene. PTPN2 played

PTPN2 is important for KRAS-driven cancer

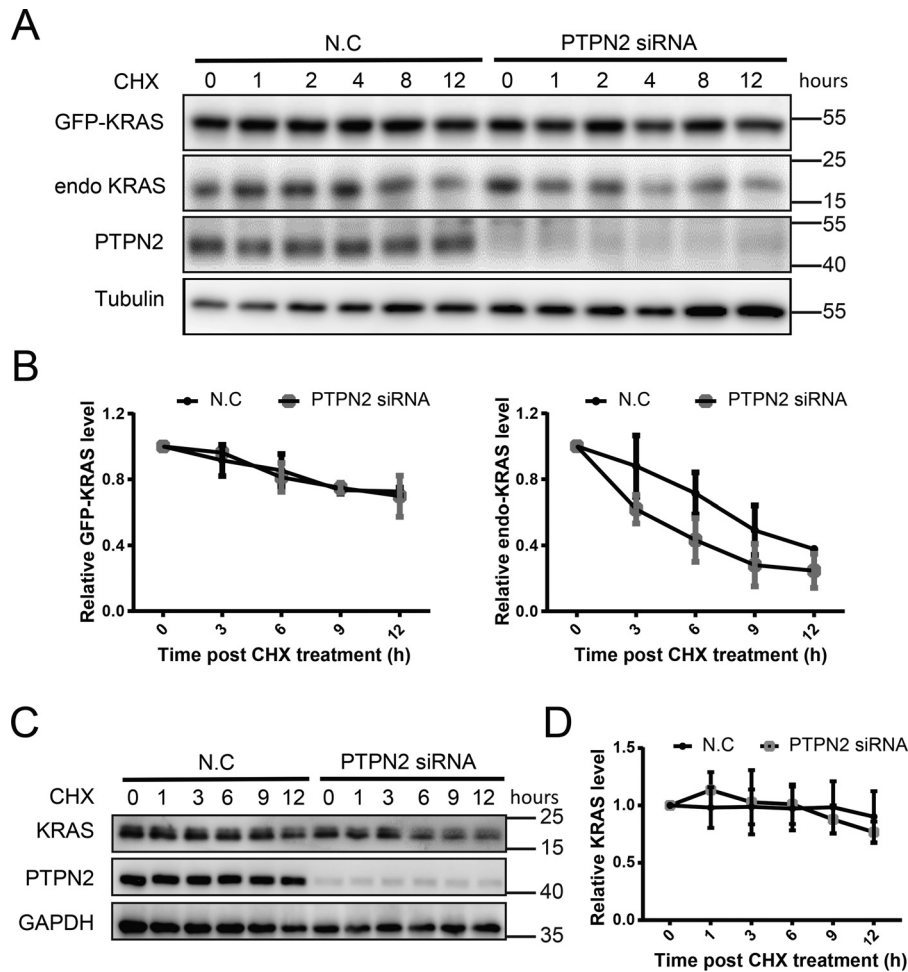


Figure 5. PTPN2 regulates the endogenous KRAS protein stability. *A*, GFP-KRAS^{G12D} HEK 293T cells were transfected with the indicated siRNA. Forty-eight h post-transfection, cells were treated with CHX (50 μ g/ml), and cell lysates were harvested at the indicated time points and analyzed by immunoblotting with the antibodies indicated. The immunoblot data are representative of two independent experiments. *B*, graphical representation of the quantification of exogenous (GFP-KRAS^{G12D}) and endogenous KRAS protein levels shown in *A* to determine protein half-life. Relative KRAS levels were determined by densitometric scanning of the representative immunoblot. The band intensity at time 0 was set as 1 (arbitrary units). *C*, H460 cells were transfected with the indicated siRNA. Forty-eight h post-transfection, cells were treated with CHX (50 μ g/ml), and cell lysates were harvested at the indicated time points and analyzed by immunoblotting with the antibodies indicated. The immunoblot data are representative of two independent experiments. *D*, graphical representation of the quantification of KRAS protein levels shown in *C* to determine protein half-life. Relative KRAS levels were determined by densitometric scanning of the representative immunoblot. The band intensity at time 0 was set as 1 (arbitrary units).

tumor-promoting functions in B-cell lymphomas, and *Ptpn2* depletion decreased murine B-cell lymphoma cell proliferation and completely abolished the cancer *in vivo* (40). It was also shown that *PTPN2* expression levels are strongly associated with prognosis in patients with glioma and glioblastoma. Patients with a high expression of *PTPN2* tend to have a poor prognosis, suggesting that *PTPN2* can promote tumor development (41). Here, we show for the first time that *PTPN2* plays a tumor-promoting function in KRAS-driven cancer.

It has been proven that KRAS is phosphorylated via Src, which alters the conformation of switch I and II regions, profoundly reducing the KRAS' binding affinity to RAF. In contrast, SHP2 dephosphorylates KRAS and thereby restores the affinity to RAF, which enhances the KRAS-mediated MAPK pathway. Inhibition of SHP2 promotes accumulation of phosphorylated KRAS and subsequently suppressing KRAS-RAF-MAPK signaling (32). Here, *PTPN2* is identified as another phosphatase that dephosphorylates KRAS and regulates the activation of KRAS and its downstream signaling.

It has been suggested that the type of mutations in KRAS may have an influence on its ability to transform and the drug responses of cancer patients. SHP2 inhibitor RMC-4550, for example, has shown a potent inhibitory effect on the cancer cell lines bearing missense mutations in KRAS at Gly-12, but not Gly-13, and Gln-61 (42). In this study, we found it is interesting that the requirement of *PTPN2* for KRAS activation is independent of the mutant *KRAS* isoforms, which included G12V (PaTu8988T), G13D (HCT-116), and Q61K (H460). Both *PTPN2* and SHP2 can dephosphorylate KRAS, but their negative regulatory signal molecules are somewhat different. The underlying mechanism requires subsequent experiments to explore.

Recently, studies have shown that *Kras*-mutant-bearing cancers display features with reduced T helper 1 cells as well as reduced infiltration of cytotoxic cells via recruiting the myeloid-derived suppressor cells, which made *Kras*-mutant tumor resistant to immune checkpoint blockade (ICB) therapy (43). One mechanism is that *Kras*-driven cancers could down-

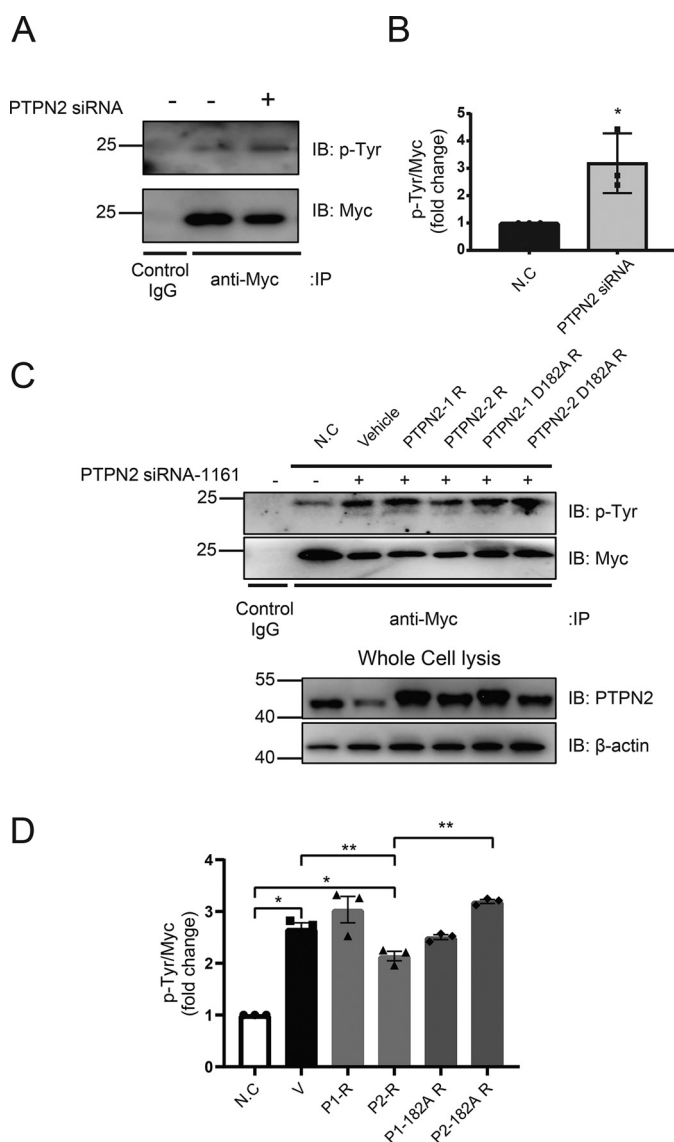


Figure 6. Effect of PTPN2 knockdown on the KRAS tyrosine phosphorylation. *A*, HEK 293T cells were transfected with the indicated plasmid and siRNA. Cells were lysed, immunoprecipitated, and immunoblotted with the indicated antibodies. The immunoblot data are representative of three independent experiments. *B*, quantitation of data in *A*. Assessment of tyrosine phosphorylation of KRAS in samples from three repeat experiments by Western blot ($n = 3$; mean \pm S.D.; two-tailed *t* test. *, $p < 0.05$). *C*, HEK 293T cells were transfected with the indicated plasmid and siRNA. Cells were lysed, immunoprecipitated (*IP*), and immunoblotted (*IB*) with the indicated antibodies. The immunoblot data are representative of three independent experiments. *D*, quantitation of data in *C*. Assessment of tyrosine phosphorylation of KRAS in samples from 3 repeat experiments by Western blot ($n = 3$; mean \pm S.D.; one-way ANOVA followed by Tukey's test. *, $p < 0.05$; **, $p < 0.01$). P1-R, PTPN2-1 R; P2-R, PTPN2-2 R; P1-182A R, PTPN2-1 D182A R; P2-182A R, PTPN2-2 D182A R.

regulate the interferon- γ (IFN- γ) and IFN- α responses, which are crucial in anti-PD-1 therapy in patients with cancer (43). It is interesting that loss of *Ptpn2* results in an increase in number and activation of CD8+ T cells, and enhancing of IFN- γ -mediated effects on antigen presentation (44, 45). Therefore *Ptpn2* has recently been identified as a novel cancer immunotherapy target in a CRISPR screening *in vivo*, where deletion of this gene increased the efficacy of immune checkpoint blockade therapy in melanoma (45). Moreover, one study has demon-

strated that myeloid cell-specific loss of *Ptpn2* promotes inflammasome activation, resulting in protection from colorectal cancer (46). Thus, inhibition of PTPN2 could suppress KRAS cancer, whereas enhancing tumor immunity.

In summary, we identified PTPN2 is a key regulator of KRAS activation and signaling transduction. The results indicate that PTPN2 may be a novel therapeutic target for KRAS-driven cancers.

Materials and methods

Cell culture

Human lung (H460 and A549), pancreatic (PaTu8988T), colon (HCT-116 and DLD-1), fibrosarcoma (HT1080), and skin (SK-MEL-30) cancer cell lines and the HEK 293T cell line were obtained from the American Type Culture Collection (ATCC) and authenticated by ATCC and DSMZ using Short Tandem Repeat profiling analysis. These cells were detected periodically to ensure mycoplasma-free cells. HCT-116 and DLD-1 cells were cultured in RPMI-1640 medium (BasalMedia, Shanghai, China); HEK 293T, H460, PaTu8988T, and A549 cells were cultured in Dulbecco's modified Eagle's medium (BasalMedia, Shanghai, China), HT-1080 and SK-MEL-30 were cultured in minimal essential medium (BasalMedia, Shanghai, China). All media were supplemented with 10% fetal bovine serum (Gibco, Carlsbad, CA, USA), 1 \times penicillin/streptomycin, and the cells were cultured in a humidified 5% CO₂ incubator at 37°C.

DNA constructs

GFP-fused KRAS^{G12D}, Myc-fused KRAS^{G12D}, PTPN2 siRNA-1161-resistant (PTPN2-Res), and catalytically inactive mutation (PTPN2-D182A) plasmids were generated as previously described (6, 47). All constructs were confirmed by DNA sequencing before use.

HEK 293T cell line stably expressing GFP-KRAS^{G12D}

HEK 293T cells were maintained in Dulbecco's modified Eagle's medium supplemented with 10% fetal bovine serum at 37°C, 5% CO₂. Transfection of GFP-KRAS^{G12D} was carried out using Lipofectamine 3000 reagent (Invitrogen) per the manufacturer's protocol. GFP-positive cells were sorted twice on a fluorescent-activated cell sorting (FACS) machine, and further placed on a 96-well flat-bottom tissue culture plate, one GFP positive cell/well. Cells were further cultured for 2 weeks, detached with trypsin-EDTA, and then cultured in a 6-well-plate. The GFP-KRAS^{G12D} expressing cell lines were used for further experiments.

siRNA screening

siRNA screening was performed in GFP-KRAS^{G12D} HEK 293T cells using a pre-aliquoted Silencer siRNA library (Dharmacon; Human ON-TARGETplus, Lafayette, CO, USA) at 25 nM final concentration. siRNAs were arrayed into 96-well-plates (CellCarrier-96, PerkinElmer, Waltham, MA, USA) in duplicate. Gene silencing was induced for 72 h via reverse transfection using RNAiMAX reagent (Invitrogen, catalog number 13778). Cells with mislocalized GFP-KRAS^{G12D} were

PTPN2 is important for KRAS-driven cancer

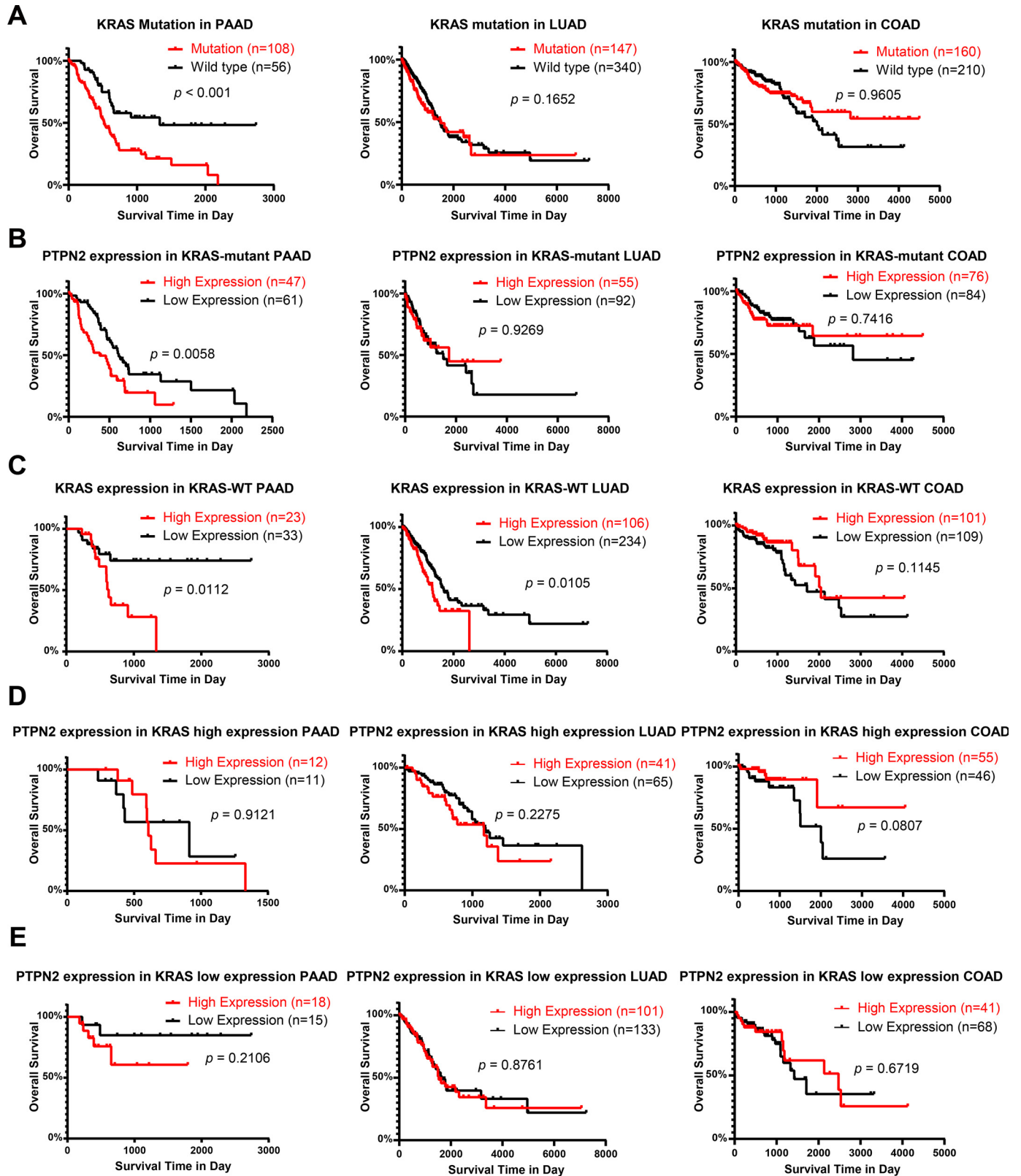


Figure 7. High level expression of PTPN2 is associated with poor prognosis of KRAS-mutant PAAD patients. A, Kaplan-Meier plots of overall survival of patients with PAAD, LUAD, or COAD stratified by KRAS mutation. B, Kaplan-Meier plots of overall survival of patients with PAAD, LUAD, or COAD stratified by PTPN2 expression in KRAS-mutant cancers. C, Kaplan-Meier plots of overall survival of patients with PAAD, LUAD, or COAD stratified by KRAS expression in KRAS-WT cancers. D, Kaplan-Meier plots of overall survival of patients with PAAD, LUAD, or COAD stratified by PTPN2 expression in KRAS high expression cancers. E, Kaplan-Meier plots of overall survival of patients with PAAD, LUAD, or COAD stratified by PTPN2 expression in KRAS low expression cancers. Data were all obtained from the TCGA database.

then screened using an Opera Phenix High-Content Screening System (PerkinElmer). Images were acquired for 17 fields with a $\times 40$ water immersion objective using the GFP-confocal mode. The siRNA was listed in Table S1.

Western blot analysis

To prepare whole-cell lysates, cells were washed twice with ice-cold phosphate-buffered saline (PBS) and lysed in SDS lysis buffer (100 mM Tris-HCl, 2% SDS, 10% glycerol, 50 mM dithiothreitol, 0.1% bromophenol blue, pH 6.8) supplemented with protease inhibitor cocktail and 2 mM phenylmethylsulfonyl fluoride. Proteins from the lysates were separated by SDS-polyacrylamide gel electrophoresis and Western blotted with the following antibodies: (a) anti-phospho-MEK1/2 (Ser-217/221) (catalog number 9121, 1:1000), anti-phospho-ERK1/2 (D13.14.4E; catalog number 4370, 1:1000), anti-GFP (catalog number 2555, 1:1000), anti-p44/42 MAPK (Erk1/2) (137F5) (catalog number 4695S, 1:1000), anti-MEK1/2 (9122; 1:1000), and anti-Myc (71D10, catalog number 2278, 1:1000) (all from Cell Signaling Technology, Danvers, MA, USA); (b) anti-KRAS (catalog number WH0003845M1, 1:1000) and anti-PTPN2 (catalog number HPA046176, 1:1000) (both from Sigma-Aldrich), anti-[EP1845Y] sodium potassium ATPase (catalog number ab76020; 1:1000, from Abcam); (c) HRP-conjugated GAPDH (catalog number HRP-6004, 1:4000), HRP-conjugated β -actin (catalog number HRP-60008, 1:4000), and HRP-conjugated α -tubulin antibody (catalog number HRP-66031, 1:4000) (all from ProteinTech, Chicago, IL, USA). The secondary antibody was anti-mouse IgG, HRP-linked antibody (Cell Signaling Technology, 1:3000; catalog number 7076) or anti-rabbit IgG, HRP-linked antibody (Cell Signaling Technology, 1:3000; catalog number 7074). The Western blots images were developed with an Amersham Imager 600 (GE Healthcare, Boston, MA, USA). Each Western blot shown is a representative of a minimum of 2 independent experiments.

Flow cytometry

The thymidine analog 5-bromo-2-deoxyuridine (BrdU) incorporation assay was performed according to the standard protocol of the manufacturer (BD Pharmingen™ BrdU Flow Kits; catalog number 559619). Cells were transfected with siRNA via reverse transfection using RNAiMAX reagent (Invitrogen, catalog number 13778) at a final concentration of 50 nM and seeded in 6-well-plates for 72 h. BrdU (10 μ M) was added and incubated further for 3 h. Then, cells were washed three times with $1\times$ PBS and fixed and permeabilized the cells with BD Cytotfix/Cytoperm Buffer. Cell were further permeabilized with Cytoperm Permeabilization Buffer Plus for 10 min on ice and re-fixed with Cytotfix/Cytoperm Buffer for 10 min on ice. After incubation with DNase for 1 h at 37°C, cells were stained with FITC-conjugated anti-BrdU antibody for 30 min at room temperature. Before detecting by flow cytometry, cells were stained with nucleolus dye 7-amino-actinomycin D for 15 min. The percentage of BrdU-positive cells was counted and reckoned by using the GraphPad Prism 5.

Apoptosis was detected and quantified using the Annexin V Apoptosis Detection Kit APC (eBioscience, Waltham, MA,

USA, catalog number 88800772). Briefly, after treatment with siRNA for 72 h, cells were harvested and washed with ice-cold PBS, and then suspended in Annexin binding buffer. Subsequently, cells were incubated with Annexin V-APC and propidium iodide for 15 min at room temperature in the dark and immediately analyzed using a BD LSRFortessa flow cytometer (BD Biosciences, Franklin Lakes, NJ, USA). Data were analyzed with the FlowJo (Tree Star) software.

siRNA-mediated knockdown of KRAS and PTPN2

Cells were transfected with siRNA via reverse transfection using Dharmafect 1 Transfection Reagent (Dharmacon, catalog number T2001-01) or RNAiMAX reagent (Invitrogen, catalog number 13778) at a final concentration of 50 nM and seeded in 6-well-plates for Western blotting or apoptosis assays and 96-well-plates for cell viability assays. Transfected cells were collected 72 h after transfection for Western blot analysis as described above, and after 72 h for the CellTiter-Glo® Luminescent Cell Viability Assay (Promega) as described below. The siRNAs were obtained from GenePharma Corporation (Shanghai, China) and the sequences used for KRAS siRNA and PTPN2 siRNA experiments are as follows: negative control, sense UUCUCCGAACGUGUCACGUTT and antisense ACGUGACACGUUCGGAGAATT; KRAS siRNA-244, sense GCCUUGACGAUACAGCUAATT and antisense UUAGCUGUAUCGUCAAGGCTT; KRAS siRNA-585, sense GGACUUAGCAAGAAGUUAUTT and antisense AUAACUUCUUGCUAAGUCCTT; KRAS siRNA-643, sense GGUGUUGAUGAUGCUCUUCUTT and antisense AGAAGGCAUCAUCAACACCTT; PTPN2 siRNA-432, Sense CAAAGGAGUUACAUCUUAATT and antisense UUAAGAUGUAAACUCCUUUGTT; and PTPN2 siRNA-1161, sense GCCUUUGAUCUUAUCCACCAATT and antisense UUGGUGAAUGAUCAAAGGCTT.

Cell viability assay

Cell viability assays were carried out using the CellTiter-Glo® Luminescent Cell Viability Assay as previously described (48). H460, PaTu8988T, HCT-116, A549, DLD-1, HT-1080, and SK-MEL-30 cells were transfected with siRNA via reverse transfection using Dharmafect 1 or RNAiMAX at a final concentration of 50 nM and seeded in regular 96-well-plates at a density of 5×10^3 to 1×10^4 cells/well. After 72 h incubation, cell viability was measured using the CellTiter-Glo reagent. The luminescence was detected using an Envision plate reader (PerkinElmer).

KRAS activity assay

KRAS activity was determined using RAS activation assay kit (EMD Millipore, 17–218, Burlington, MA, USA) according to the manufacturer's protocol with minor modifications. Briefly, cells were lysed in Pierce IP Lysis Buffer (Thermo Scientific, catalog number 87788) supplemented with protease and phosphatase inhibitors (Roche Applied Science), and lysates were further incubated with 5 μ g of RAF-1 RBD-agarose beads for 8 h at 4°C. After washing the agarose beads three times with Pierce IP Lysis Buffer, the activated KRAS (GTP-RAS) bound to RAF-1 RBD-agarose beads was released by the addition of SDS lysis buffer. Finally, samples were subjected to Western

PTPN2 is important for KRAS-driven cancer

blotting analysis as previously described and blots were probed using an anti-KRAS antibody (Sigma, 1:1000).

Immunoprecipitation and immunoblotting

HEK 293T cells were transfected with siRNA via reverse transfection using Dharmafect 1 at a final concentration of 50 nM and seeded in regular 6-well-plates at a density of 1×10^6 cells/well. After 24 h incubation, cells were transiently transfected the Myc-tagged KRAS^{G12D} plasmid using the Lipo6000 Transfection Reagent (Beyotime, Shanghai, China, catalog number C0526) per the manufacturer's protocol and further cultured for 48 h. Cells were lysed in Pierce IP Lysis Buffer supplemented with protease and phosphatase inhibitors (Roche), and lysates were further incubated with 10 μ g of anti-Myc tag antibody (agarose) (Abcam, Cambridge, England, UK, catalog number ab1253) or IgG-agarose beads (Abcam, catalog number ab104155) for 8 h at 4 °C. After washing the agarose beads three times with Pierce IP Lysis Buffer, the Myc-tagged-KRAS bound to agarose beads was released by the addition of SDS lysis buffer. Finally, samples were subjected to Western blotting analysis as previously described and blots were probed using an anti-phosphotyrosine antibody (Cell Signaling Technology, catalog number 9411, 1:1000) or anti-Myc antibody (Cell Signaling Technology, 1:1000).

KRAS protein stability

GFP-KRAS^{G12D} HEK 293T cells and H460 were transfected with siRNA via reverse transfection using RNAiMAX at a final concentration of 50 nM and seeded in regular 12-well-plates at a density of 2.5×10^5 cells/well. Forty-eight h later fresh medium containing cycloheximide (50 μ g/ml) was added. At the indicated time intervals, cells were washed twice with ice-cold PBS and lysed in SDS lysis buffer supplemented with protease inhibitor cocktail and 2 mM PMSF. Finally, samples were subjected to Western blotting analysis as previously described.

Analyses of the association of the KRAS mutation, KRAS expression, and PTPN2 expression in PAAD, LUAD, or COAD clinical outcome

The KRAS mutation, PTPN2 expression, and clinical information of KRAS-related cancers were extracted from the TCGA database. This dataset contains survival data with clinical information, KRAS mutations, KRAS mRNA expression counts, and PTPN2 mRNA expression counts. The groups were separated by the mean expression level of the group. Overall survival stratified by expression levels of the gene of interest was evaluated using Kaplan–Meier analysis, and comparisons between groups were evaluated using log-rank tests. $p < 0.05$ was considered statistically significant.

Statistical analysis

Data of continuous variables are presented as mean \pm SD. Comparisons between treatments were analyzed by one-way ANOVA followed by Tukey's test using GraphPad Prism 5. $p < 0.05$ was deemed statistically significant.

Data availability

All data relevant to this study are included within this manuscript.

Acknowledgements—We thank Yi Jin, Qianqian Zhang, Jing Lu, Zheng Ruan, Yan Sheng, and Shuai Han for technical assistance.

Author contributions—Z. H., M. L., B. J., P. L., and R. R. conceptualization; Z. H., M. L., D. L., Y. T., R. Z., and Z. X. data curation; Z. H., D. L., R. Z., Z. X., and P. W. formal analysis; Z. H., M. L., and D. L. investigation; Z. H., M. L., D. L., Y. T., R. Z., Z. X., P. W., B. J., P. L., and R. R. methodology; Z. H. writing-original draft; M. L., P. L., and R. R. writing-review and editing; Y. T. resources; B. J. and R. R. funding acquisition; P. L. and R. R. supervision.

Funding and additional information—This work was supported by Key Program of Natural Science Foundation of China Grant 81530006 (to R. R.), Natural Science Foundation of China Grants 81870112 (to R. R.), 81970134 (to P. L.), and 81770171 (to B. J.), Shanghai Collaborative Innovation Program on Regenerative Medicine and Stem Cell Research Grant 2019CXJQ01 (to R. R.), the Samuel Waxman Cancer Research Foundation (to R. R.), and the Innovative research team of high-level local universities in Shanghai.

Conflict of interest—The authors declare no conflict of interest.

Abbreviations—The abbreviations used are: PM, plasma membrane; FTase, farnesyltransferases; GGTase, geranylgeranyltransferase; FTI, FTase inhibitor; PTPN2, protein-tyrosine phosphatase non-receptor type 2; CHX, cycloheximide; NC, negative control; PAAD, pancreatic adenocarcinoma; LUAD, lung adenocarcinoma; COAD, colorectal adenocarcinoma; MAPK, mitogen-activated protein kinase; IFN- γ , interferon- γ ; HEK, human embryonic kidney; HRP, horseradish peroxidase; ANOVA, analysis of variance; GAPDH, glyceraldehyde-3-phosphate dehydrogenase.

References

1. Malumbres, M., and Barbacid, M. (2003) RAS oncogenes: the first 30 years. *Nat. Rev. Cancer* **3**, 459–465 [CrossRef Medline](#)
2. Cox, A. D., Fesik, S. W., Kimmelman, A. C., Luo, J., and Der, C. J. (2014) Drugging the undruggable RAS: Mission possible? *Nat. Rev. Drug Discov.* **13**, 828–851 [CrossRef Medline](#)
3. Li, S., Balmain, A., and Counter, C. M. (2018) A model for RAS mutation patterns in cancers: finding the sweet spot. *Nat. Rev. Cancer* **18**, 767–777 [CrossRef Medline](#)
4. Jackson, E. L., Willis, N., Mercer, K., Bronson, R. T., Crowley, D., Montoya, R., Jacks, T., and Tuveson, D. A. (2001) Analysis of lung tumor initiation and progression using conditional expression of oncogenic K-ras. *Genes Dev.* **15**, 3243–3248 [CrossRef Medline](#)
5. Johnson, L., Mercer, K., Greenbaum, D., Bronson, R. T., Crowley, D., Tuveson, D. A., and Jacks, T. (2001) Somatic activation of the K-ras oncogene causes early onset lung cancer in mice. *Nature* **410**, 1111–1116 [CrossRef Medline](#)
6. Parikh, C., Subrahmanyam, R., and Ren, R. (2007) Oncogenic NRAS, KRAS, and HRAS exhibit different leukemogenic potentials in mice. *Cancer Res.* **67**, 7139–7146 [CrossRef Medline](#)
7. Hanahan, D., and Weinberg, R. A. (2011) Hallmarks of cancer: the next generation. *Cell* **144**, 646–674 [CrossRef Medline](#)

8. Pylyayeva-Gupta, Y., Grabocka, E., and Bar-Sagi, D. (2011) RAS oncogenes: weaving a tumorigenic web. *Nat. Rev. Cancer* **11**, 761–774 [CrossRef Medline](#)
9. Pecot, C. V., Wu, S. Y., Bellister, S., Filant, J., Rupaimoole, R., Hisamatsu, T., Bhattacharya, R., Maharaj, A., Azam, S., Rodriguez-Aguayo, C., Nagaraja, A. S., Morelli, M. P., Gharpure, K. M., Waugh, T. A., Gonzalez-Villasana, V., Zand, B., Dalton, H. J., Kopetz, S., Lopez-Berestein, G., Ellis, L. M., and Sood, A. K. (2014) Therapeutic silencing of KRAS using systemically delivered siRNAs. *Mol. Cancer Ther.* **13**, 2876–2885 [CrossRef Medline](#)
10. Yuan, T. L., Fellmann, C., Lee, C. S., Ritchie, C. D., Thapar, V., Lee, L. C., Hsu, D. J., Grace, D., Carver, J. O., Zuber, J., Luo, J., McCormick, F., and Lowe, S. W. (2014) Development of siRNA payloads to target KRAS-mutant cancer. *Cancer Discov.* **4**, 1182–1197 [CrossRef Medline](#)
11. Kamerkar, S., LeBleu, V. S., Sugimoto, H., Yang, S., Ruivo, C. F., Melo, S. A., Lee, J. J., and Kalluri, R. (2017) Exosomes facilitate therapeutic targeting of oncogenic KRAS in pancreatic cancer. *Nature* **546**, 498–503 [CrossRef Medline](#)
12. Patricelli, M. P., Janes, M. R., Li, L. S., Hansen, R., Peters, U., Kessler, L. V., Chen, Y., Kucharski, J. M., Feng, J., Ely, T., Chen, J. H., Firdaus, S. J., Babbar, A., Ren, P., and Liu, Y. (2016) Selective inhibition of oncogenic KRAS output with small molecules targeting the inactive state. *Cancer Discov.* **6**, 316–329 [CrossRef Medline](#)
13. Janes, M. R., Zhang, J., Li, L. S., Hansen, R., Peters, U., Guo, X., Chen, Y., Babbar, A., Firdaus, S. J., Darjania, L., Feng, J., Chen, J. H., Li, S., Li, S., Long, Y. O., Thach, C., Liu, Y., Zariw, A., Ely, T., Kucharski, J. M., Kessler, L. V., Wu, T., Yu, K., Wang, Y., Yao, Y., Deng, X., Zarrinkar, P. P., Brehmer, D., Dhanak, D., Lorenzi, M. V., Hu-Lowe, D., Patricelli, M. P., Ren, P., and Liu, Y. (2018) Targeting KRAS mutant cancers with a covalent G12C-specific inhibitor. *Cell* **172**, 578–589.e17 [CrossRef Medline](#)
14. Fehrenbacher, N., Tojal da Silva, I., Ramirez, C., Zhou, Y., Cho, K. J., Kuchay, S., Shi, J., Thomas, S., Pagano, M., Hancock, J. F., Bar-Sagi, D., and Philips, M. R. (2017) The G protein-coupled receptor GPR31 promotes membrane association of KRAS. *J. Cell Biol.* **216**, 2329–2338 [CrossRef Medline](#)
15. Adhikari, H., and Counter, C. M. (2018) Interrogating the protein interactomes of RAS isoforms identifies PIP5K1A as a KRAS-specific vulnerability. *Nat. Commun.* **9**, 3646 [CrossRef Medline](#)
16. Kowalski, J. R., Bhaduri, A., Zehnder, A. M., Neela, P. H., Che, Y., Wozniak, G. G., and Khavari, P. A. (2019) The functional proximal proteome of oncogenic Ras includes mTORC2. *Mol. Cell* **73**, 830–844.e12 [CrossRef Medline](#)
17. Temraz, S., Mukherji, D., and Shamseddine, A. (2015) Dual inhibition of MEK and PI3K pathway in KRAS and BRAF mutated colorectal cancers. *Int. J. Mol. Sci.* **16**, 22976–22988 [CrossRef Medline](#)
18. Kinsey, C. G., Camolotto, S. A., Boespflug, A. M., Guillen, K. P., Foth, M., Truong, A., Schuman, S. S., Shea, J. E., Seipp, M. T., Yap, J. T., Burrell, L. D., Lum, D. H., Whisenant, J. R., Gilcrease, G. W., 3rd, Cavalieri, C. C., Rehbein, K. M., Cutler, S. L., Affolter, K. E., Welm, A. L., Welm, B. E., Scaife, C. L., Snyder, E. L., and McMahon, M. (2019) Protective autophagy elicited by RAF→MEK→ERK inhibition suggests a treatment strategy for RAS-driven cancers. *Nat. Med.* **25**, 620–627 [CrossRef Medline](#)
19. Rinehart, J., Adjei, A. A., Lorusso, P. M., Waterhouse, D., Hecht, J. R., Natale, R. B., Hamid, O., Varterasian, M., Asbury, P., Kaldjian, E. P., Gulyas, S., Mitchell, D. Y., Herrera, R., Sebolt-Leopold, J. S., and Meyer, M. B. (2004) Multicenter phase II study of the oral MEK inhibitor, CI-1040, in patients with advanced non-small-cell lung, breast, colon, and pancreatic cancer. *J. Clin. Oncol.* **22**, 4456–4462 [CrossRef](#)
20. Blumenschein, G. R., Jr., Smit, E. F., Planchard, D., Kim, D. W., Cadranet, J., De Pas, T., Dunphy, F., Udud, K., Ahn, M. J., Hanna, N. H., Kim, J. H., Mazieres, J., Kim, S. W., Baas, P., Rappold, E., Redhu, S., Puskis, A., Wu, F. S., and Janne, P. A. (2015) A randomized phase II study of the MEK1/MEK2 inhibitor trametinib (GSK1120212) compared with docetaxel in KRAS-mutant advanced non-small-cell lung cancer (NSCLC)dagger. *Ann. Oncol.* **26**, 894–901 [CrossRef Medline](#)
21. Jänne, P. A., van den Heuvel, M. M., Barlesi, F., Cobo, M., Mazieres, J., Crinò, L., Orlov, S., Blackhall, F., Wolf, J., Garrido, P., Poltoratskiy, A., Mariani, G., Ghiorghiu, D., Kilgour, E., Smith, P., Kohlmann, A., Carlile, D. J., Lawrence, D., Bowen, K., and Vansteenkiste, J. (2017) Selumetinib plus docetaxel compared with docetaxel alone and progression-free survival in patients with KRAS-mutant advanced non-small cell lung cancer: The SELECT-1 randomized clinical trial. *JAMA* **317**, 1844–1853 [CrossRef Medline](#)
22. Hancock, J. F. (2003) Ras proteins: different signals from different locations. *Nat. Rev. Mol. Cell Biol.* **4**, 373–384 [CrossRef Medline](#)
23. Hancock, J. F., and Parton, R. G. (2005) Ras plasma membrane signalling platforms. *Biochem. J.* **389**, 1–11 [CrossRef Medline](#)
24. Wu, M., Huang, J., Zhang, J., Benes, C., Jiao, B., and Ren, R. (2017) N-Arachidonoyl dopamine inhibits NRAS neoplastic transformation by suppressing its plasma membrane translocation. *Mol. Cancer Ther.* **16**, 57–67 [CrossRef Medline](#)
25. Cox, A. D., Der, C. J., and Philips, M. R. (2015) Targeting RAS membrane association: back to the future for anti-RAS drug discovery? *Clin. Cancer Res.* **21**, 1819–1827 [CrossRef Medline](#)
26. Whyte, D. B., Kirschmeier, P., Hockenberry, T. N., Nunez-Oliva, I., James, L., Catino, J. J., Bishop, W. R., and Pai, J. K. (1997) K- and N-Ras are geranylgeranylated in cells treated with farnesyl protein transferase inhibitors. *J. Biol. Chem.* **272**, 14459–14464 [CrossRef Medline](#)
27. Lobell, R. B., Omer, C. A., Abrams, M. T., Bhimnathwala, H. G., Brucker, M. J., Buser, C. A., Davide, J. P., deSolms, S. J., Dinsmore, C. J., Ellis-Hutchings, M. S., Kral, A. M., Liu, D., Lumma, W. C., Machotka, S. V., Rands, E., Williams, T. M., Graham, S. L., Hartman, G. D., Oliff, A. I., Heimbrook, D. C., and Kohl, N. E. (2001) Evaluation of farnesyl:protein transferase and geranylgeranyl:protein transferase inhibitor combinations in preclinical models. *Cancer Res.* **61**, 8758–8768 [Medline](#)
28. Dekker, F. J., Rocks, O., Vartak, N., Menninger, S., Hedberg, C., Balamurugan, R., Wetzel, S., Renner, S., Gerauer, M., Schölermann, B., Rusch, M., Kramer, J. W., Rauh, D., Coates, G. W., Brunsfeld, L., Bastiaens, P. I., and Waldmann, H. (2010) Small-molecule inhibition of APT1 affects Ras localization and signaling. *Nat. Chem. Biol.* **6**, 449–456 [CrossRef Medline](#)
29. Chandra, A., Grecco, H. E., Pisupati, V., Perera, D., Cassidy, L., Skoulidis, F., Ismail, S. A., Hedberg, C., Hanzal-Bayer, M., Venkitaraman, A. R., Wittinghofer, A., and Bastiaens, P. I. (2011) The GDI-like solubilizing factor PDEδ sustains the spatial organization and signalling of Ras family proteins. *Nat. Cell Biol.* **14**, 148–158 [CrossRef Medline](#)
30. Zimmermann, G., Papke, B., Ismail, S., Vartak, N., Chandra, A., Hoffmann, M., Hahn, S. A., Triola, G., Wittinghofer, A., Bastiaens, P. I., and Waldmann, H. (2013) Small molecule inhibition of the KRAS-PDEδ interaction impairs oncogenic KRAS signalling. *Nature* **497**, 638–642 [CrossRef Medline](#)
31. Schmick, M., Vartak, N., Papke, B., Kovacevic, M., Truxius, D. C., Rossmannek, L., and Bastiaens, P. I. H. (2014) KRas localizes to the plasma membrane by spatial cycles of solubilization, trapping and vesicular transport. *Cell* **157**, 459–471 [CrossRef Medline](#)
32. Kano, Y., Gebregiworgis, T., Marshall, C. B., Radulovich, N., Poon, B. P. K., St-Germain, J., Cook, J. D., Valencia-Sama, I., Grant, B. M. M., Herrera, S. G., Miao, J., Raught, B., Irwin, M. S., Lee, J. E., Yeh, J. J., Zhang, Z. Y., Tsao, M. S., Ikura, M., and Ohh, M. (2019) Tyrosyl phosphorylation of KRAS stalls GTPase cycle via alteration of switch I and II conformation. *Nat. Commun.* **10**, 224 [CrossRef Medline](#)
33. Guerra, C., Mijimolle, N., Dhawahir, A., Dubus, P., Barradas, M., Serrano, M., Campuzano, V., and Barbacid, M. (2003) Tumor induction by an endogenous K-ras oncogene is highly dependent on cellular context. *Cancer Cell* **4**, 111–120 [CrossRef Medline](#)
34. Hingorani, S. R., Petricoin, E. F., Maitra, A., Rajapakse, V., King, C., Jacobetz, M. A., Ross, S., Conrads, T. P., Veenstra, T. D., Hitt, B. A., Kawaguchi, Y., Johann, D., Liotta, L. A., Crawford, H. C., Putt, M. E., Jacks, T., Wright, C. V., Hruban, R. H., Lowy, A. M., and Tuveson, D. A. (2003) Preinvasive and invasive ductal pancreatic cancer and its early detection in the mouse. *Cancer Cell* **4**, 437–450 [CrossRef Medline](#)
35. Cool, D. E., Tonks, N. K., Charbonneau, H., Walsh, K. A., Fischer, E. H., and Krebs, E. G. (1989) cDNA isolated from a human T-cell library encodes a member of the protein-tyrosine-phosphatase family. *Proc. Natl. Acad. Sci. U.S.A.* **86**, 5257–5261 [CrossRef Medline](#)
36. Bothur, E., Raifer, H., Haftmann, C., Stittrich, A. B., Brustle, A., Brenner, D., Bollig, N., Bieringer, M., Kang, C. H., Reinhard, K., Camara, B., Huber,

PTPN2 is important for KRAS-driven cancer

- M., Visekruna, A., Steinhoff, U., Repenning, A., Bauer, U. M., Sexl, V., Radbruch, A., Sparwasser, T., Mashreghi, M. F., Wah Mak, T., and Lohoff, M. (2015) Antigen receptor-mediated depletion of FOXP3 in induced regulatory T-lymphocytes via PTPN2 and FOXP1. *Nat. Commun.* **6**, 8576 [CrossRef Medline](#)
37. Wiede, F., Dudakov, J. A., Lu, K. H., Dodd, G. T., Butt, T., Godfrey, D. I., Strasser, A., Boyd, R. L., and Tiganis, T. (2017) PTPN2 regulates T cell lineage commitment and $\alpha\beta$ versus $\gamma\delta$ specification. *J. Exp. Med.* **214**, 2733–2758 [CrossRef Medline](#)
38. Wiede, F., Sacirbegovic, F., Leong, Y. A., Yu, D., and Tiganis, T. (2017) PTPN2-deficiency exacerbates T follicular helper cell and B cell responses and promotes the development of autoimmunity. *J. Autoimmun.* **76**, 85–100 [CrossRef Medline](#)
39. Kleppe, M., Lahortiga, I., El Chaar, T., De Keersmaecker, K., Mentens, N., Graux, C., Van Roosbroeck, K., Ferrando, A. A., Langerak, A. W., Meijerink, J. P., Sigaux, F., Haferlach, T., Wlodarska, I., Vandenberghe, P., Soulier, J., and Cools, J. (2010) Deletion of the protein tyrosine phosphatase gene PTPN2 in T-cell acute lymphoblastic leukemia. *Nat. Genet.* **42**, 530–535 [CrossRef Medline](#)
40. Young, R. M., Polsky, A., and Refaeli, Y. (2009) TC-PTP is required for the maintenance of MYC-driven B-cell lymphomas. *Blood* **114**, 5016–5023 [CrossRef Medline](#)
41. Wang, P. F., Cai, H. Q., Zhang, C. B., Li, Y. M., Liu, X., Wan, J. H., Jiang, T., Li, S. W., and Yan, C. X. (2018) Molecular and clinical characterization of PTPN2 expression from RNA-seq data of 996 brain gliomas. *J. Neuroinflammation* **15**, 145 [CrossRef Medline](#)
42. Nichols, R. J., Haderk, F., Stahlhut, C., Schulze, C. J., Hemmati, G., Wildes, D., Tzitzilonis, C., Mordec, K., Marquez, A., Romero, J., Hsieh, T., Zaman, A., Olivas, V., McCoach, C., Blakely, C. M., Wang, Z., Kiss, G., Koltun, E. S., Gill, A. L., Singh, M., Goldsmith, M. A., Smith, J. A. M., and Bivona, T. G. (2018) RAS nucleotide cycling underlies the SHP2 phosphatase dependence of mutant BRAF-, NF1- and RAS-driven cancers. *Nat. Cell Biol.* **20**, 1064–1073 [CrossRef Medline](#)
43. Liao, W., Overman, M. J., Boutin, A. T., Shang, X., Zhao, D., Dey, P., Li, J., Wang, G., Lan, Z., Li, J., Tang, M., Jiang, S., Ma, X., Chen, P., Katkhuda, R., Korhaisarn, K., Chakravarti, D., Chang, A., Spring, D. J., Chang, Q., Zhang, J., Maru, D. M., Maeda, D. Y., Zebala, J. A., Kopetz, S., Wang, Y. A., and DePinho, R. A. (2019) KRAS-IRF2 axis drives immune suppression and immune therapy resistance in colorectal cancer. *Cancer Cell* **35**, 559–572.e57 [CrossRef Medline](#)
44. Scharl, M., Hruz, P., and McCole, D. F. (2010) Protein tyrosine phosphatase non-receptor Type 2 regulates IFN- δ -induced cytokine signaling in THP-1 monocytes. *Inflammatory Bowel Dis.* **16**, 2055–2064 [CrossRef](#)
45. Manguso, R. T., Pope, H. W., Zimmer, M. D., Brown, F. D., Yates, K. B., Miller, B. C., Collins, N. B., Bi, K., LaFleur, M. W., Juneja, V. R., Weiss, S. A., Lo, J., Fisher, D. E., Miao, D., Van Allen, E., Root, D. E., Sharpe, A. H., Doench, J. G., and Haining, W. N. (2017) *In vivo* CRISPR screening identifies Ptpn2 as a cancer immunotherapy target. *Nature* **547**, 413–418 [CrossRef Medline](#)
46. Spalinger, M. R., Manzini, R., Hering, L., Riggs, J. B., Gottier, C., Lang, S., Atrott, K., Fettelschoss, A., Olomski, F., Kündig, T. M., Fried, M., McCole, D. F., Rogler, G., and Scharl, M. (2018) PTPN2 regulates inflammasome activation and controls onset of intestinal inflammation and colon cancer. *Cell Rep.* **22**, 1835–1848 [CrossRef Medline](#)
47. Zhao, H., Liu, P., Zhang, R., Wu, M., Li, D., Zhao, X., Zhang, C., Jiao, B., Chen, B., Chen, Z., and Ren, R. (2015) Roles of palmitoylation and the KIKK membrane-targeting motif in leukemogenesis by oncogenic KRAS4A. *J. Hematol. Oncol.* **8**, 132 [CrossRef Medline](#)
48. Ning, N., Yu, Y., Wu, M., Zhang, R., Zhang, T., Zhu, C., Huang, L., Yun, C. H., Benes, C. H., Zhang, J., Deng, X., Chen, Q., and Ren, R. (2018) A novel microtubule inhibitor overcomes multidrug resistance in tumors. *Cancer Res.* **78**, 5949–5957 [Medline](#)